

Radio-loud and Radio-quiet X-ray Binaries: LSI+61°303 in Context

Maria Massi

Max Planck Institut für Radioastronomie, Auf dem Hügel 69, D-53121 Bonn, Germany

Abstract. The three basic ingredients - a spinning compact object, an accretion disc and a collimated relativistic jet - make microquasars a galactic scaled-down version of the radio-loud AGN. That explains the large interest attributed to this new class of objects, which up to now consists of less than 20 members. Microquasars belong to the much larger class of X-ray binary systems, where there exists a compact object together with its X-ray emitting accretion disc, but the relativistic jet is missing. When does an X-ray binary system evolve into a microquasar? Ideal for studying such kind of a transition is the periodic microquasar LSI +61°303 formed by a compact object accreting from the equatorial wind of a Be star and with more than one event of super-critical accretion and ejection along the eccentric orbit. For ejections at periastron passage the relativistic electrons suffer severe inverse Compton losses by upscattering the UV photons of the Be star at high energy : At periastron passage Gamma-ray emission has been observed, whereas radio outbursts have never been observed in 20 years of radio flux monitoring. For ejections displaced from periastron passage the losses are less severe and radio outbursts are observed. The radio emission mapped on scales from a few AU to hundreds of AU shows a double-sided relativistic ($\beta = 0.6c$) S-shaped jet, similar to the well-known precessing jet of SS 433.

1. Introduction

Since the beginning of the 1980s radio-galaxies, quasars, Seyferts, QSO etc. all are simply classified as AGNs (“Active Galactic Nuclei”) because the “energy-engine” is thought to be the same: A super-massive black hole accreting from its host galaxy. AGNs having radio-emitting lobes or jets are called radio-loud, the others are called radio-quiet (Ulrich et al. 1997).

In an X-ray binary system the “energy-engine” is a compact object of a few solar masses accreting from the companion star. Up to now there are almost 250 known X-ray binaries (Liu 2000). Only a small percentage of them (<10%) show evidence of a radio-jet and therefore are radio loud applying the same definition as for the AGNs. The radio loud X-ray binaries subclass (Fig. 1) includes together with the microquasars—objects where high resolution radio interferometric techniques have shown the presence of collimated jets (Mirabel et al. 1992)—also unresolved radio sources with a flat spectrum. This spectrum can arise from the combination of emission from optically thick and thin regions of an expanding continuous jet (Hjellming & Johnston 1988; Fender 2004) as has been shown by the discovery of a continuous jet for the flat-spectrum source Cygnus X-1 (Stirling et al. 2001).

Besides the first radio loud X-ray binary system SS433, discovered by chance in 1979 (Margon 1984), the others have been discovered mostly in the last ten years and now are considered as an ideal, nearby laboratory for studying the processes of accretion and ejection around black holes.

More generally speaking, the class of the X-ray binaries is formed by stellar systems of two stars with very different natures: a normal star (acting as mass donor) and a compact object (the accretor) that can be either a neutron star or a black hole (White et al 1996). The normal star orbits around the compact object and therefore the infalling material has some angular momentum (J), which prevents it from falling directly into the accretor. The stream of matter orbits the compact object with

a radius determined by J and the mass of the compact object (M_x). The angular momentum is redistributed by the viscosity: Some of the material takes angular momentum and spreads outwards, whereas other material spirals inwards. In this way a disk is created from the initial ring of matter (Longair 1994; King 1996). Gradually, the matter drifts inwards until it reaches the last stable orbit. The viscosity has two effects: Beside the transport of the angular-momentum it also acts as a frictional force resulting in the dissipation of heat. The amount of friction depends on how fast the gas orbits around the compact object. It reaches its maximum at the inner disk, where the matter is heated up to quite high temperatures (tens of millions of degrees), producing the strong thermal X-ray radiation giving the name “X-ray binaries” to this class of objects.

In the case of a low vertical magnetic field threading the disk the plasma pressure dominates the magnetic field pressure and the differentially rotating disk bends the magnetic field, which is passively wound up (Meier et al. 2001). Due to the compression of the magnetic field lines the magnetic pressure may become larger than the gas pressure at the surface of the accretion disk, where the density is lower. At this point the gas follows the twisted magnetic field lines, creating two spinning flows. These extract angular momentum from the surface of the disk (magnetic braking) and enhance the radial accretion. The avalanching material further pulls the deformed magnetic field with it and afterwards magnetic reconnection may happen (Matsumoto et al. 1996). The thickness of the disc is fundamental in this magneto-rotational process, or better the extent of the poloidal magnetic field frozen into the disc (Meier 2001; Meier et al. 2001; Maccarone 2004). No radio jet is associated at X-ray binaries in High/soft states, where the X-ray spectrum is dominated by a geometrically thin (optically thick) accretion disc (Shakura & Sunyaev 1973). Whereas, numerical results show a jet being launched from an inner geometrically thick portion of the accretion disc existing (coronal

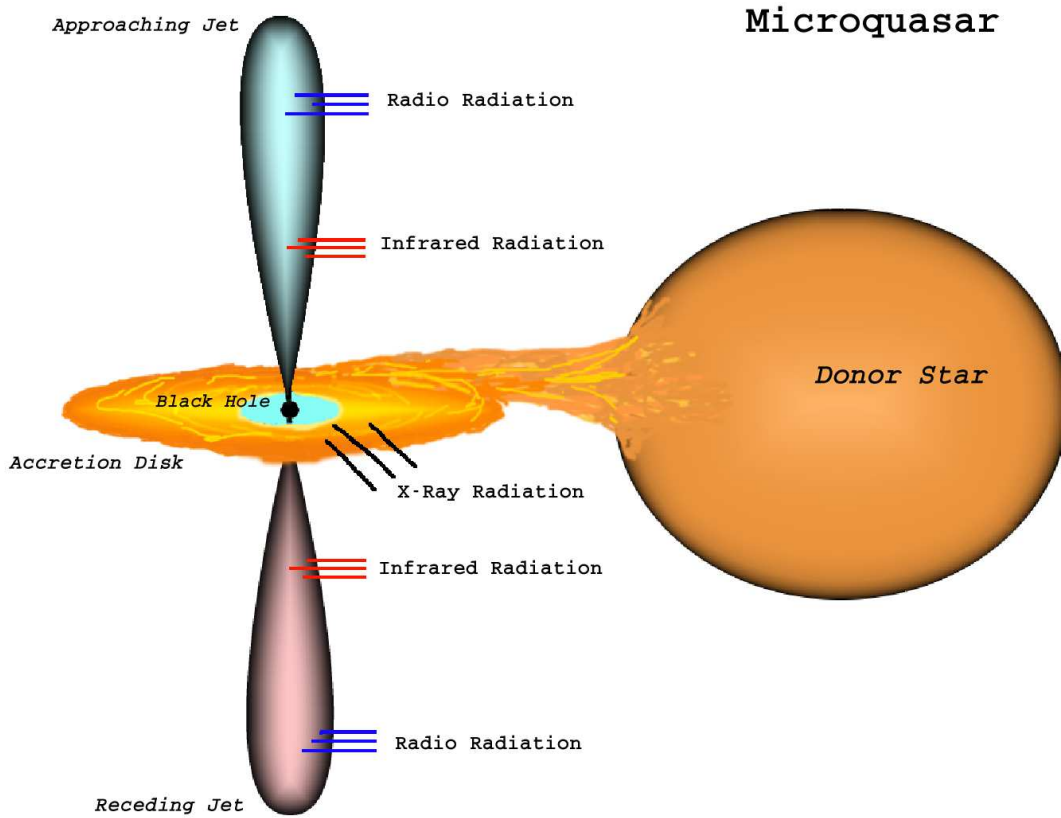


Fig. 1. The basic components of a microquasar - a spinning compact object, an accretion disk and a collimated relativistic jet. The compact object, of a few solar masses, accretes from a normal star in orbital motion around it. The mass of the compact object can be determined by studying the periodical shift of the optical spectral lines of the normal star and establishes, if it is a neutron star or a black hole. The inner part of the disk emits X-rays. The inner radius, three times the Schwarzschild radius, is a few tens of kilometers, the outer radius a factor 10^3 larger (the figure is not to scale). Due to magneto-rotational instabilities part of the disk is propelled into a relativistic jet, studied at high resolution with radio interferometric techniques. In some microquasars, like SS433 and LS I+61°303, the jet is precessing. If the precession causes the jet to be aligned toward the earth the large variable doppler boosting mimics the variability of Blazars and the microquasar in this case is called microblazar.

flow/ADAF) when the X-ray binaries are in their low/hard state (Meyer et al. 2000; Meier 2001).

Among the X-ray binaries an ideal source to study the transition to the microquasar phase is LS I +61°303 because it is the only known periodic microquasar.

2. The LS I +61°303 system

LS I +61°303 is the only object of this class showing variations in X-rays (Leahy 2001), optical wavelengths in both continuum (Maraschi & Treves 1981) and line radiation (Zamanov & Martí 2000; Liu et al. 2000) and at radio wavelengths with a period equal to the orbital one; the most accurate value of the orbital period is that resulting from radio observations, equal to 26.496 days (Gregory & Taylor 1978; Taylor & Gregory 1982; Gregory 2002). The fit performed on near infrared data by Martí and Paredes (1995) produced high values for the eccentricity ($e \sim 0.7-0.8$) confirmed by optical observations (Casares et al. 2004). The lower limit to i , the angle formed by the axis of the orbit and the line of sight is 38° (Hutchings & Crampton 1981; Massi et al. 2001; Massi 2004). The phase at the pe-

riatron passage is $\Phi=0.2$ with the phase referred to the time $t_0 = \text{JD } 2443366.775$, the date of the first radio detection of the system (Gregory & Taylor 1978).

Ultraviolet spectroscopy of LS I +61°303 by Hutchings & Crampton (Hutchings & Crampton 1981) indicates that the normal star is a main sequence B0-B0.5 star ($L \sim 10^{38} \text{ erg sec}^{-1}$, $T_{\text{eff}} \approx 2.6 \cdot 10^4 \text{ K}$). The optical spectrum is that of a rapidly spinning Be star. Together with the usual high velocity (1000 km s^{-1}) low density wind at high latitudes typical for OB stars, Be stars have a dense and slow ($< 100 \text{ km s}^{-1}$) disk-like wind around the equator (Waters et al. 1988). Equatorial mass loss, due to an interplay of the high rotation and of internal pulsations of the star, is highly variable and in some cases periodical. This is the case for LS I +61°303, where periodical variations of the mass loss from the Be star have been proved by a modulation of H α emission line with a period of almost 4 years (Zamanov and Martí 2000).

The most reliable method to determine the nature of the compact object is the study, as usual in binary systems, of the changing radial velocity of the normal companion during its orbit. The amplitude (K_c) of the radial velocity variations and the

period (P_{orb}) of the system define a quantity, called the “mass function” (Charles & Wagner 1996), f , which depends on the inclination i of the orbit, the masses M_X and M of the accretor and its normal companion:

$$f = \frac{P_{orb} K_c^3}{2\pi G} = \frac{M_X^3 \sin^3 i}{(M_X + M)^2}$$

where G is the gravitational constant.

Once the inclination, i , and the mass of the companion, M , are known one can solve for M_X .

Rhoades & Ruffini (1974) by taking the most extreme equation of state that produces the maximum critical mass of a neutron star, established the upper limit of $3.2 M_\odot$. This absolute maximum mass provides a decisive method of observationally distinguishing neutron stars from black holes. The problem with LS I +61°303 is the large range for the mass function allowed by the parameter uncertainties. Optical observations (Casares et al. 2004) give the mass function f in the range $0.003 < f < 0.027$. The upper limit for f , with $i=38$ and $M = 18 M_\odot$ gives $M_X < 3.8 M_\odot$. Therefore the nature of the accretor is still an open issue (Massi 2004).

3. Radio emission

The greatest peculiarity of LS I +61°303 are its periodic radio outbursts with $P=26.496$ days (Gregory 2002). In Fig.2 a typical radio light curve is shown. The decay of the outburst agrees with that expected for an adiabatically expanding cloud of synchrotron-emitting relativistic electrons (Taylor & Gregory 1984). However, that model alone fails to fit the peaks at different frequencies: the flat spectrum during the late portion of the rise in flux density can be reproduced, if together with the adiabatic expansion losses also a continuous ejection of particles lasting two days is taken into account (Paredes et al 1991).

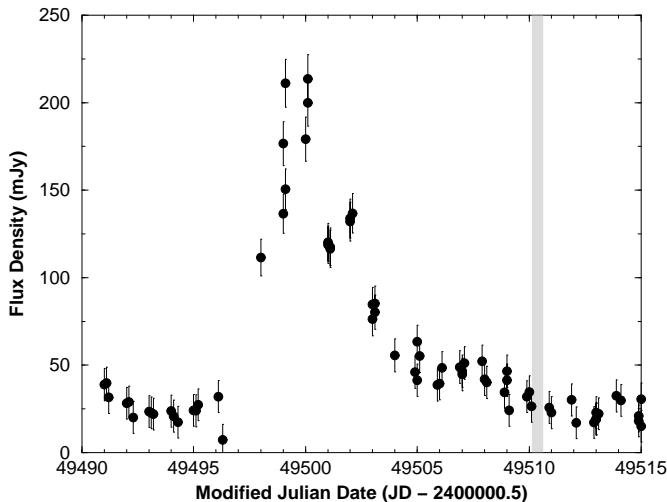


Fig. 2. Radio light curve of LS I +61°303 obtained with the GBI at 8.4 GHz (Strickman et al. 1998). The shaded area indicates the time interval during the EVN observation of Fig. 4 (figure in Massi et al. 2001).

The amplitude of each outburst is not randomly varying, but itself periodic with a periodicity of 4.6 years correlated with the mass loss of the Be star (sect. 2) (Gregory 1999, 2002; Zamanov & Martí 2000). Also, the orbital phase Φ at which the outbursts occur is modulated (Gregory et al. 1999) and varies in the interval 0.45–0.95 (Paredes et al. 1990). The Φ at periastron passage is 0.2. Therefore one of the fundamental questions concerning the periodic radio outbursts of LS I +61°303 has been: Why are the radio outbursts shifted with respect to the periastron passage?

4. The two peak accretion model

In order to explain the association between LS I +61°303 and the gamma-ray source 2CG 135+01/3EG J0241+6103, Bosch-Ramon and Paredes (2004) have proposed a numerical model based on inverse Compton scattering. The relativistic electrons in the jet are exposed to stellar photons (external Compton) as well as to synchrotron photons (synchrotron self Compton). The model considers accretion variations along the orbit and predicts a gamma-ray peak at periastron passage where the accretion is higher. EGRET data show indeed a gamma-ray peak at $\Phi=0.2$ (Fig. 3) and catastrophic inverse Compton losses might explain the absence of radio emission at periastron. Therefore, to explain the observed periodic radio outbursts in the phase interval 0.45–0.95 a second accretion/ejection event must occur.

Taylor et al. (1992) and Martí & Paredes (1995) have shown that for accretion along an eccentric orbit the accretion rate $\dot{M} \propto \frac{\rho_{wind}}{v_{rel}^3}$, (where ρ_{wind} is the density of the Be star wind and v_{rel} is the relative speed between the accretor and wind) develops two peaks: the highest peak corresponds to the periastron passage (highest density), while the second peak occurs when the drop in the relative velocity v_{rel} compensates the decrease in density (because of the inverse cube dependence). Martí & Paredes (1995) have shown that during both peaks the accretion rate is above the Eddington limit and therefore one expects that matter is ejected twice within the 26.496 days interval. Martí & Paredes have found that variations of Be star wind velocity produce a variation in the orbital phase of the second peak. At this second accretion peak the compact object is far enough away from the Be star, so that the inverse Compton losses are small and electrons can propagate out of the orbital plane. Then an expanding double radio source should be observed, which in fact has been observed by VLBI and MERLIN.

5. A precessing jet

The first VLBI observation resolving the source, made by Massi and collaborators (1993; $\Phi=0.74$) revealed a complex morphology (Fig.4 bottom) not easy to interpret. Two components (at P.A. $\approx 30^\circ$) are separated by 0.9 mas, corresponding to 1.8 AU at a distance of 2 kpc. The two components are inside an extended and sensibly rotated structure at P.A. $\approx 135^\circ$). What is the nature of this complex morphology? Is the envelope an older expanding jet, previously ejected, because of precession, at another angle? Taylor and collaborators (2000; $\Phi=0.69$) performing VLBI observations in combination with the HALCA

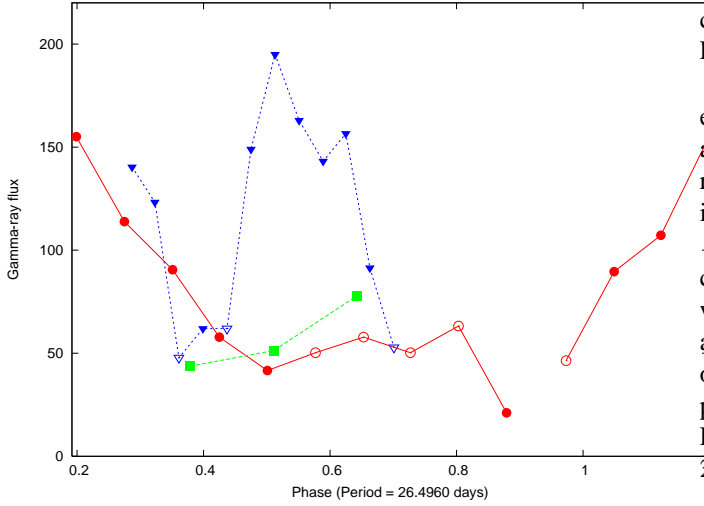


Fig. 3. EGRET data (Tavani et al. 1998) folded with the orbital/radio period $P = 26.4960$ days. The plot begins at periastron passage $\Phi \approx 0.2$ and shows the follow-up of the gamma-ray emission along one full orbit. At epoch 2450334JD (i.e. circles in the plot, with empty circles indicating upper limits) the orbit has been well sampled at all phases: A clear peak is centered at periastron passage 0.2 and 1.2. At a previous epoch (2449045JD; triangles in the plot, with empty triangles indicating upper limits) the sampling is uncomplete, still the data show an increase toward ($\Phi \approx 0.3$) periastron passage and a peak at $\Phi \approx 0.5$. The 3 squares refer to a third epoch (2449471JD). The emission is suggested to be produced via inverse Compton scattering of stellar photons (Taylor et al. 1992, 1996) and of synchrotron photons (Bosch-Ramon & Paredes 2004) by the relativistic electrons of the jet. The ejection is predicted to occur twice along the orbit, one always at periastron passage and the second at a varying orbital phase (Martí and Paredes 1995). Relativistic electrons ejected at $\Phi=0.2$ suffer severe Compton losses: radio outbursts never occur at periastron. Radio outbursts occur in the orbital phase interval 0.45-0.95 (Paredes et al. 1990). The gamma-ray peak at $\Phi \approx 0.5$ could be associated to a such second ejection. However, no radio data are available to calculate energy budget/losses of the relativistic electrons (figure in Massi et al. 2004b).

orbiting antenna mapped a curved structure of 4 mas (8 AU) reminiscent ”of the precessing radio jet seen in SS433”.

EVN observations (Massi et al 2001; $\Phi=0.92$) at a scale of up to tens of AU show an elongation clearly in one direction without any ambiguity (see Fig. 4-Top). The observed flux density of the approaching (S_a) and the receding (S_r) jet are a function of θ , the angle between the jet and the line of sight, by the Doppler factor: $\delta_{a,r} = [\Gamma(1 \mp \beta \cos \theta)]^{-1}$, where $\Gamma = (1 - \beta^2)^{-1/2}$ is the Lorentz factor and βc the jet velocity (Mirabel & Rodriguez 1999). The observed flux density of the approaching jet will be boosted and that of the receding jets de-boosted as $S_{a,r} = S_{a,r}^{k-\alpha}$, where α is the spectral index of the emission ($S_\nu \propto \nu^{+\alpha}$) and k is 2 for a continuous jet and 3 for discrete condensations. That creates an asymmetry between the two jet components. The receding attenuated jet can even disappear because of the sensitivity limit of the image. In this

case the jet appears only on one side as it is the case for the EVN image.

The first of two consecutive MERLIN observations (Massi et al. 2004; $\Phi=0.68$) shows a double S-shaped jet extending to about 200 AU on both sides of a central source (Fig. 5 a). The receding jet is attenuated but still above the noise limit of the image.

The precession suggested from the first MERLIN image becomes evident in the second one ($\Phi=0.71$), shown in Fig.5 b, where a new feature is present oriented to the North-East at a position angle (PA) of 67° . It is likely that the morphology of the source is S-shaped because the only visible jet appears indeed bent. The Northwest-Southeast jet of Fig.5 a has a PA= 124° . Therefore a quite large rotation has occurred in only 24 hours.

The appearance of successive ejections of a precessing jet with ballistic motion of each ejection is a curved path, that depending on the modality of the expansion and therefore on the adiabatic losses seems to be a “twin-corkscrew” or a simply S-shaped pattern (Hjellming & Johnston 1988; Crocker et al. 2002) Can we distinguish in our data the single ejections in ballistic motion?

We have split the MERLIN data of each epoch into blocks of a few hours and created separate images (Fig. 6) (i.e. Fig. 5a is the combination of the first two blocks: 6a and 6b; Fig. 5b a combination of 6c and 6d). We see that the Eastern bent structure present in Fig. 5a is the result of a combination of an old ejection A (Fig. 6a), already displaced 120 mas from the core, and a new ejection B (Fig. 6b). After 19 hours (Fig. 6c) the feature B is reduced to 2σ and a new ejection C, at a different PA with respect to B, appears. In Fig. 6d, 6 hours later, little rotation of the PA is compatible with $\Delta \text{PA}_{(B-C)}/3$ of the previous image.

From the maps it is evident that the projection of the jet on the sky plane is changing, but how much is the variation of θ ? If the jet velocity is the same for all ejections, the change of the ratio $\frac{S_a}{S_r} = \left(\frac{1+\beta \cos \theta}{1-\beta \cos \theta} \right)^{k-\alpha}$ is due to variations of θ . Adopting values of $k = 2$, $\alpha = -0.5$ and the a value of $\beta = 0.6$ we obtain: $\theta_A < 90^\circ$, $\theta_B < 80^\circ$ and for the C ejection in Fig. 6 c, $\theta_C < 68^\circ$.

6. Conclusions

The main points of our review on the characteristics of the source LS I +61°303 in the frame of the two-peak accretion/ejection model are:

1. It is still an open issue whether the compact object in this system is a neutron star or a black hole. In fact, taking into account the uncertainty in inclination, mass of the companion and the mass function, the existence of a black hole cannot be ruled out.
2. The radio jet at a scale of hundreds of AU quite strongly changes its morphology in short intervals (within 24 hours), evolving from an initial double-sided jet into an one-sided jet. This variation corresponds to a reduction of more than 10° in the angle between the jet and the line of sight. This new alignment severely Doppler de-boosts the counter-jet.

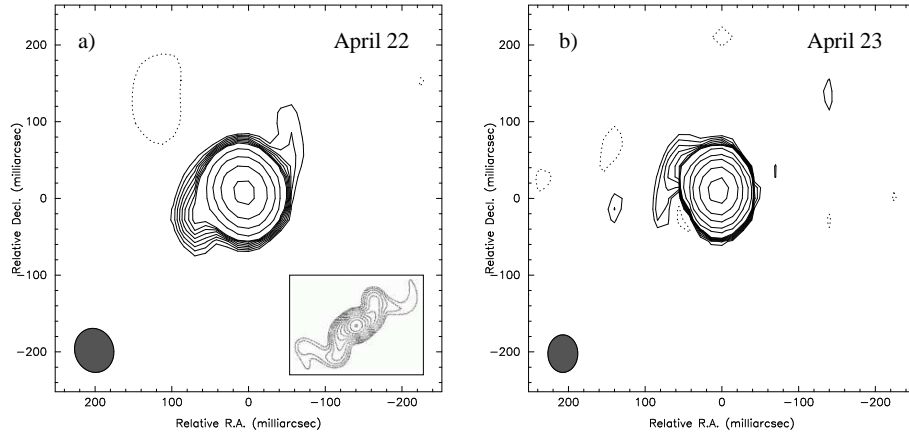


Fig. 5. a) MERLIN image of LS I +61°303 at 5 GHz obtained on 2001 April 22. North is up and East is to the left. The synthesized beam has a size of 51×58 mas, with a PA of 17° . The contour levels are at $-3, 3, 4, 5, 6, 7, 8, 9, 10, 20, 40, 80$, and 160σ , being $\sigma=0.14$ mJy beam $^{-1}$. The S-shaped morphology strongly recalls the precessing jet of SS 433, whose simulated radio emission (Fig. 6b in Hjellming & Johnston 1988) is given in the small box. b) Same as before but for the April 23 run. The synthesized beam has a size of 39×49 mas, with a PA of -10° . The contour levels are the same as those used in the April 22 image but up to 320σ , with $\sigma=0.12$ mJy beam $^{-1}$ (figure in Massi et al. 2004).

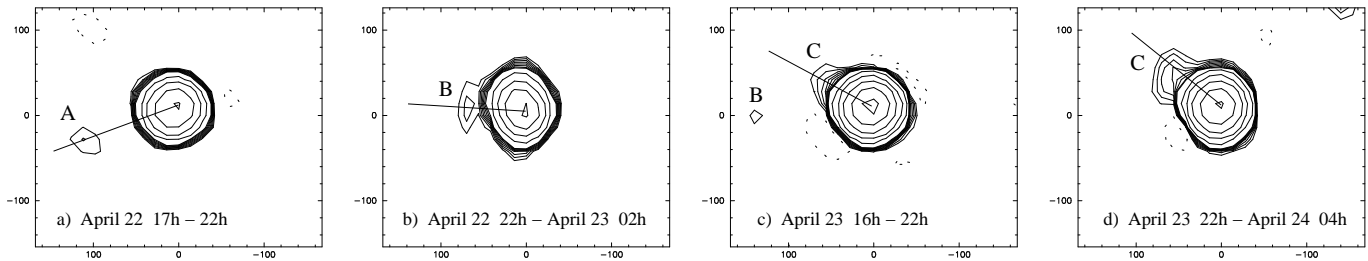


Fig. 6. MERLIN images of LS I +61°303 of 2001 April 22 and April 23. The data set of each epoch has been split into two blocks (i.e. Fig. 5a is the combination of the first two blocks: 6a and 6b; Fig. 5b a combination of 6c and 6d). A convolving beam of 40 mas has been used in all images for better display. The first contour represents the 3σ level in all images except for c), where we start from the 2σ level to display the faint B component. The rms noises are $\sigma=0.13$ mJy beam $^{-1}$, $\sigma=0.20$ mJy beam $^{-1}$, $\sigma=0.13$ mJy beam $^{-1}$, and $\sigma=0.15$ mJy beam $^{-1}$, respectively. The PA of the ejections is indicated by a bar (figure in Massi et al. 2004).

Further observational evidence for a precessing jet is recognizable even at AU scales.

3. The same population of relativistic electrons emitting radio-synchrotron radiation may upscatter - by inverse Compton processes - ultraviolet stellar photons and produce gamma-ray emission. For ejections at the periastron passage gamma-ray flares are expected, but because of severe Compton losses no radio flares, as indeed the data seem to indicate.

We conclude that as precession and variable doppler boosting are the causes of the rapid change in the radio-morphology, precession and variable doppler boosting are likely to produce gamma-ray variations at short time scales. The amplification due to the Doppler factor for Compton scattering of stellar photons by the relativistic electrons of the jet is $\delta^{3-2\alpha}$ (where $\alpha < 0$), and therefore higher than that for synchrotron emission, i.e. $\delta^{2-\alpha}$ (Kaufman Bernadó et al. 2002). LS I +61°303 becomes therefore the ideal laboratory to test the recently proposed model for microblazars with INTEGRAL and MERLIN observations now and by AGILE and GLAST in the future.

Acknowledgements. It is a pleasure to thank Karl Menten and Jürgen Neidhöfer for careful reading of the manuscript and valuable comments and discussions.

References

- Bosch-Ramon, V. & Paredes, J. M. 2004, A&A, accepted [astro-ph/0407016]
 Casares, J., Ribas, I., Paredes, J. M., & Martí, J. 2004, A&A, submitted
 Charles, P.A. & Wagner, R.M. 1996, Sky & telescope, May, 38
 Crocker, M., Davis, R., J., Spencer, R., E., Eyres, S., P., S., Bode, M., F., Skopal, A. 2002, MNRAS, 335, 1100
 Fender, R. P 2004, Compact Stellar X-Ray Sources, (W. H. G. Lewin & M. van der Klis, Cambridge University Press) in press [astro-ph/0303339]
 Gregory, P.C. 1999, ApJ, 520, 361
 Gregory, P.C. 2002, ApJ, 575, 427
 Gregory, P.C., Peracaula, M., & Taylor, A.R. 1999, ApJ, 520, 376
 Gregory, P.C., & Taylor, A.R. 1978, Nature, 272, 70
 Hutchings, J.B. & Crampton, D. 1981, PASP, 93, 486
 King, A. 1996, X-Ray Binaries, ed. W.H.G. Lewin, J. van Paradijs and M. van der Klis (Cambridge University Press, Cambridge) 419

- Liu, Q.Z., van Paradijs, J., & van den Heuvel, E.P.J. 2000, *A&AS*, 147, 25
- Longair, M.S. 1994, *High Energy Astrophysics*, Vol. 2 (Cambridge University Press, Cambridge) 135
- Hjellming, R. M., & Johnston, K. J. 1988, *ApJ*, 328, 600
- Kaufman Bernadó, M.M., Romero, G.E. & Mirabel, I.F. 2002, *A&A*, 385, L10.
- Leahy, D. A. 2001 *A&A*, 380, 516
- Liu, Q.Z., Hang, H.R., Wu, G.J., Chang, J. & Zhu, Z.X. 2000, *A&A*, 359, 646
- Maccarone, T. J. 2004, *MNRAS* 351, 1049
- Maraschi, L. & Treves, A. 1981, *MNRAS*, 194, 18
- Margon, B.A. 1984, *ARA&A*, 22, 507
- Martí, J., & Paredes, J.M. 1995, *A&A*, 298, 151
- Massi, M. 2004, *A&A*, 422, 267
- Massi, M., Paredes, J.M., Estalella, R., & Felli, M. 1993, *A&A*, 269, 249
- Massi, M., Ribó, M., Paredes, J.M., Peracaula, M., & Estalella, R. 2001, *A&A*, 376, 217.
- Massi, M., Ribó, M., Paredes, J. M., Garrington, S. T., Peracaula, M., & Martí, J. 2004, *A&A*, 414, L1
- Massi, M., Ribó, M., Paredes, J. M., Garrington, S. T., Peracaula, M., & Martí, J. 2004b, *proc. International Symposium on High Energy Gamma-Ray Astronomy*, July 26-30 2004, Heidelberg, Germany.
- Matsumoto, R., Uchida, Y., Hirose, S., Shibata, K., Hayashi, M.R., Ferrari, A., & Bodo, G. 1996, *ApJ*, 461, 115
- Meier, D. L. 2001 *ApJ*, 548, 9
- Meier, D. L., Koide, S., & Uchida, Y. 2001, *Science*, 291, 84
- Meyer, F., Liu, B.F. & Meyer-Hofmeister, E. 2000, *A&A* 354, L67
- Mirabel, I.F., & Rodríguez, L.F. 1999, *ARA&A*, 37, 409
- Mirabel, I. F., Rodríguez, L. F., Cordier, B., Paul, J. & Lebrun, F. 1992, *Nature*, 358, 215
- Paredes, J. M., Estalella, R. & Rius, A. 1990 *A&A*, 232, 337
- Paredes, J. M., Martí, J., Estalella, R. & Sarrate, J. 1991, *A&A*, 248, 124
- Rhoades, C.E. & Ruffini, R. 1974 *Physical Review Lett.*, 32, 324
- Shakura, N.I., & Sunyaev, R.A. 1973, *A&A*, 24, 337
- Stirling, A.M., Spencer, R.E., De la Force, C.J., et al. 2001, *MNRAS*, 327, 1273
- Strickman, M.S., Tavani, M., Coe, M.J., et al. 1998, *ApJ*, 497, 419
- Tavani, M., Kniffen, D., Mattox, J.R., Paredes, J.M., & Foster, R.S. 1998, *ApJ*, 497, L81
- Taylor, A.R., & Gregory, P.C. 1982, *ApJ*, 255, 210
- Taylor, A.R., Kenny, H.T., Spencer, R.E., & Tzioumis, A. 1992, *ApJ*, 395, 268
- Taylor, A.R., Young, G., Peracaula, M., Kenny, H.T., & Gregory, P.C. 1996, *A&A*, 305, 817
- Ulrich, M., Maraschi, L., & Urry, C.M. 1997, *ARAA*, 35, 445
- Waters, L.B.F.M., van den Heuvel, E.P., Taylor, A.R., Habets, G.M.H.J., & Persi, P. 1988, *A&A*, 198, 200.
- White, N.E., Nagase, F. & Parmar, A.N. 1996, *X-Ray Binaries* (W.H.G. Lewin, J. van Paradijs and M. van der Klis, Cambridge University Press, Cambridge) 33
- Zamanov, R.K. & Martí, J. 2000, *A&A*, 358, L55

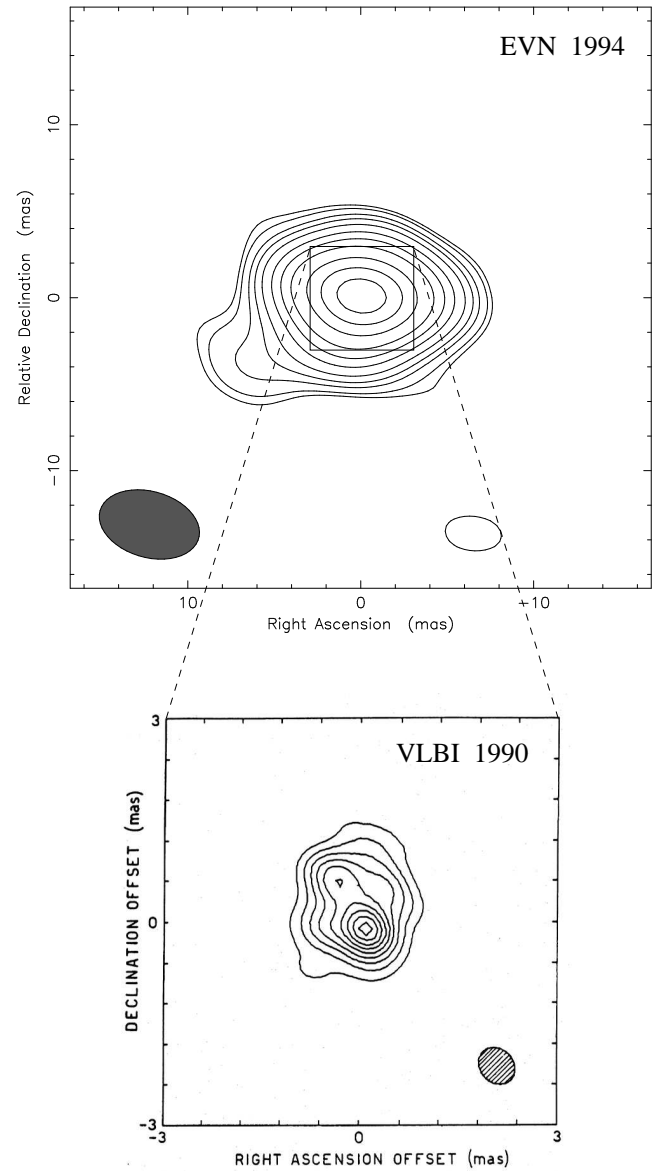


Fig. 4. Bottom: VLBI observation of LSI +61°303 at 6cm. The telescopes involved were those at Effelsberg (Germany), Westerbork (Netherlands), Medicina (Italy), Onsala (Sweden) and VLA (New Mexico, USA). The observation, lasting 14 hours, was performed during a slow decay of a large (> 250 mJy) outburst. The beam is 0.6×0.5 mas. The peak flux density is 36 mJy/beam. The lowest contour is 15% of the peak and the increment is of 10%. Top: EVN uniform weighted map of LSI +61°303 at 6 cm. The telescopes involved were those at Effelsberg, Medicina, Noto (Italy) and Onsala. The contours are at $-3, 3, 4, 6, 8, 11, 16, 22, 30, 45, 60$ and 75 times the r.m.s. noise of $0.28 \text{ mJy beam}^{-1}$. The filled ellipse in the bottom-left corner represents the FWHM of the synthesized beam, which is $5.9 \text{ mas} \times 3.8 \text{ mas}$ at a P.A. of 74.2° (figure in Massi et al. 2001).